

Localization of Unmanned Aerial Vehicles in Corridor Environments using Deep Learning

Ram Prasad Padhy, Shahzad Ahmad, Sachin Verma, Pankaj Kumar Sa, *Member, IEEE*,
Sambit Bakshi, *Member, IEEE*

Abstract—Vision-based pose estimation of Unmanned Aerial Vehicles (UAV) in unknown environments is a rapidly growing research area in the field of robot vision. The task becomes more complex when the only available sensor is a static single camera (monocular vision). In this regard, we propose a monocular vision assisted localization algorithm, that will help a UAV to navigate safely in indoor corridor environments. Always, the aim is to navigate the UAV through a corridor in the forward direction by keeping it at the center with no orientation either to the left or right side. The algorithm makes use of the RGB image, captured from the UAV front camera, and passes it through a trained deep neural network (DNN) to predict the position of the UAV as either on the left or center or right side of the corridor. Depending upon the divergence of the UAV with respect to the central bisector line (CBL) of the corridor, a suitable command is generated to bring the UAV to the center. When the UAV is at the center of the corridor, a new image is passed through another trained DNN to predict the orientation of the UAV with respect to the CBL of the corridor. If the UAV is either left or right tilted, an appropriate command is generated to rectify the orientation. We also propose a new corridor dataset, named NITRCorrV1, which contains images as captured by the UAV front camera when the UAV is at all possible locations of a variety of corridors. An exhaustive set of experiments in different corridors reveal the efficacy of the proposed algorithm.

Index Terms—UAV; Pose Estimation; Robot Vision; Monocular Vision; Localization; Central Bisector Line; DNN;



1 INTRODUCTION

IN recent years, Unmanned Aerial Vehicles (UAV) equipped with a single or multiple cameras have gained huge popularity in computer vision research domain due to their unique ability to present a scene from an aerial perspective. Nowadays, UAVs are predominantly used in many fields, such as aerial surveillance, military applications, inspection of disaster-hit areas or earthquake affected buildings, precision agriculture, movie making, bridge inspection, and many more. However, an accurate localization algorithm is essential in carrying out these tasks autonomously with absolute aplomb. In most of the outdoor environments, Global Positioning System (GPS) helps in obtaining the pose of the UAV and thus helps in autonomous navigation [1]. On the contrary, unreliability or complete unavailability of GPS in most of the indoor environments makes the task of pose estimation very complex.

Several solutions, such as Simultaneous Localization and Mapping (SLAM) [2], [3], [4], Parallel Tracking and Mapping (PTAM) [5], stereo vision *etc.* have been proposed for indoor autonomous navigation of robots. In SLAM and PTAM, laser range finders, RGB-D sensors or a single camera are generally used to construct the 3D model of the surrounding environment. At any instant, the position of the robot on the map can be easily inferred for autonomous navigation.

However, these tracking based systems require real-time heavy computation for constructing the map making them more suitable for ground robots as compared to aerial systems. In the case of stereo vision, depth is estimated by constructing the disparity map from stereo images [6], [7], [8]. However, these systems fail spectacularly in textureless environments, such as walls where it is very difficult to obtain features for disparity calculation. Hence, stereo based systems cannot be implemented in the case of corridor environments. Moreover, most of the available UAVs in the market are equipped with a single camera, and hence stereo vision solution is not practical in general.

In this paper, we present a monocular vision assisted method for localization and subsequently safe navigation of a UAV in corridor environments. The UAV in motion is required to avoid side-wise collision with the side-walls as well as should cease motion to avoid collision with the front wall, present at the end of the corridor. Our navigation algorithm takes input from the UAV front camera, which is a static pinhole camera. To achieve our goal, the UAV is required to localize itself in the unknown corridor. Our aim is to keep the UAV at the center of the corridor with no orientation either to the left or right. Once the algorithm safely localizes the UAV inside the corridor, it can navigate in the forward direction with minimal chance of collision. However, different external (e.g. wind) and internal hindrances (e.g. rotor turbulence) may deviate the direction during UAV flight. Hence, the algorithm continuously monitors the pose of the UAV during its flight and generates the necessary command in case there is any deviation from the actual path.

- R. P. Padhy, S. Ahmad, S. Verma, P. K. Sa and S. Bakshi are with the Department of Computer Science and Engineering, National Institute of Technology, Rourkela 769008, India. (E-mail: ramprasad.nitr@gmail.com, shahzadnit@gmail.com, jsrsachinverma999@gmail.com, sambitbakshi@gmail.com/bakshisambit@ieee.org, pankajksa@nitrrkl.ac.in)

The advantage of this method over the existing PTAM and SLAM based systems is that it does not require real-time 3D construction of the environment, thus computation is very low. Also, the proposed localization algorithm can act as an additive to tracking based systems and significantly lower the computation time. Hence, the proposed algorithm is more suitable for UAV systems, where the reaction time is very low as compared to ground robots. Furthermore, unlike the stereo-based systems, this method is not dependent on feature extraction, hence can very well work in texture-less environments, such as corridors.

The principal contributions of this paper are as follows:

- (a) We propose a model, which uses two similar deep neural networks (DNN) to localize the UAV in unknown indoor corridor environments. The first neural network is responsible for predicting the deviation of the UAV in terms of translation from the center of the corridor, whereas the second neural network predicts the orientation of the UAV, when the UAV is approximately at the center.
- (b) The algorithm generates necessary control commands to keep the UAV along the central bisector line of the corridor and continuously monitors the position to rectify any deviation.
- (c) We propose a new corridor dataset, NITRCorrV1 [9], which contains images as captured from the UAV front camera from different positions of a number of corridors, having varying dimensions and intensity exposure. As per the best of our knowledge, we are the first ones to propose such a dataset, which contains the deviation of the UAV in terms of translational and rotational parameters.
- (d) We show the efficacy of the proposed algorithm in real-time UAV navigation flights inside indoor corridors.

Rest of the paper is organized as follows. Section 2 presents prior research in the field of UAV navigation. Section 3 provides an overview of the proposed methodology. Section 4 presents the detailed process of our custom dataset creation followed by a thorough elaboration on the proposed DNN based autonomous navigation algorithm in Section 5. Section 6 provides the experimental results of our proposed model along with the results on real-time UAV navigation experiments. Finally, the concluding remarks are given in Section 7.

2 RELATED WORK

The research work in the field of UAV navigation has progressed quite significantly in the recent past. The prior work in the field of autonomous UAV navigation can be categorized into two main fields depending on the type of sensors used; (a) Navigation using proximity sensors, and (b) Navigation using vision sensors

Navigation using Proximity Sensors: Proximity sensors, such as LIDARs, ultrasonic sensors *etc.* usually sense the obstacle in the vicinity with the help of infrared rays or electromagnetic radiations [10], [11], [12]. Cruz *et al.* used the proximity sensors installed on a UAV to model the obstacle locations as well as the goal point in the environment [13]. A SLAM system on Android platform is developed by Chen *et al.* with the help of readings from the Inertial Measurement Unit (IMU) and ultrasonic sensors [2]. A laser-guided system is proposed by Stubblebine *et al.* ,

which also uses LIDAR data to map the surrounding environment [14]. Roberts *et al.* developed a UAV navigation model, which employed a Kalman filter over the data from ultrasonic sensors to estimate the best path at each location on the basis of observation density, which is estimated from a predefined map of the environment [15]. Although researchers have used proximity sensors to sense obstacles, these are not best suited for UAV navigation. High weight and difficulty in installation on a UAV make them infeasible in most of the cases of autonomous UAV navigation.

Navigation using Vision Sensors: Cameras are lightweight and low power consuming sensors, and hence is the ideal solution to detect obstacles in case of autonomous UAV navigation. In stereo vision (two cameras), triangulation geometry is used to obtain the disparity map from common feature points of the two camera views [6], [7], [8]. However, power constraint of the UAV system demands for a better solution, such as the use of a single camera (monocular vision). Monocular vision processing is more challenging as compared to stereo vision because of the absence of depth information. These systems usually employ visual odometry and optical flow to sense obstacles in unknown environments [5], [16], [17], [18], [19], [20]. He *et al.* used the IMU readings along with the data from a monocular camera to model the ego-motion parameters [21]. Sa *et al.* proposed a Kalman filter based PTAM algorithm using the inputs from a static single camera [5]. Few researchers have stressed upon the use of vanishing point from corridor images to navigate in indoor environments [22], [23]. Kim and Chen [24], and Padhy *et al.* [25] in their respective works have developed DNN based systems, that are trained on corridor datasets, to predict the next command for autonomous UAV navigation in indoor corridors. An Extended Kalman filter based monocular SLAM system was developed by Engel *et al.* to approximate the UAV position in the surrounding environment [3], [4]. A learning-based UAV navigation algorithm based on optical flow was developed by Wang *et al.* [19]. Bill *et al.* developed a system to detect obstacles in a few indoor scenarios, such as closed rooms, corridors and staircases [26]. A dead reckoning and histogram voting scheme for UAV navigation was developed by the researchers from Czech Technical University [27]. Few papers have stressed upon the use of visual keypoints and their scale change with the movement of the UAV towards the obstacle to predict the distance from a moving UAV [17], [18], [28].

Our current work uses a DNN based model that takes inputs from the UAV front camera to measure the translational as well as rotational deviation of the UAV inside a corridor. These deviations are rectified throughout the process of UAV navigation to localize the UAV safely. Unlike other neural network based UAV navigation methods inside the corridor [24], [25], that give predictions in terms of flight commands, our model predicts the approximate deviations of the UAV from a safe path. We also proposed a new corridor dataset to accomplish the task.

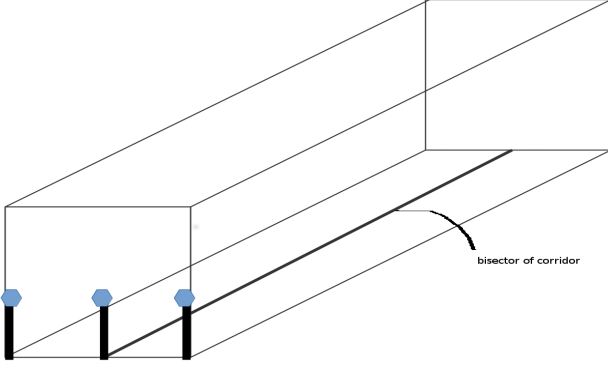


Fig. 1: Central bisector line of a corridor.

3 OVERVIEW OF THE SOLUTION STRATEGY

Our goal is to autonomously navigate a UAV in indoor corridors without any collision either with the side walls or with the front wall at the end of the corridor. The real-time data from the UAV front camera acts as input to our vision-based navigation algorithm. The algorithm first forwards one image frame through a trained regression network to measure the translational deviation of the UAV from an imaginary line, known as the central bisector line (CBL) of the corridor (Figure 1). This line runs on the middle of the floor across the whole length of the corridor and is parallel to the side walls. It may be noted that there does not exist any such line in real-world corridor environments; rather it is an imaginary line, which is used as a reference to measure the deviation of the UAV from the center of the corridor. Depending on the deviation of the UAV with respect to the CBL, a suitable command is generated to bring the UAV to the center of the corridor. Again, another image frame is forwarded through a similar trained regression network to measure the orientation from the CBL. This variation in orientation, if any, is rectified by generating a suitable control command. Once, the UAV is aligned with the CBL, it navigates in the forward direction. The process of rectifying the translational and rotational deviation continues across the whole length of the corridor, as the UAV may be subjected to different external (e.g. wind) or internal (e.g. rotor turbulence) factors, which have the potential to deviate it from a straight line path.

4 DATASET CREATION

There exist many indoor datasets([24], [29], [30]) for the task of UAV navigation. However, none of them provides ground truth values in terms of deviation with respect to the CBL of the corridor, which according to us plays a significant role for localization of a UAV inside corridor environments. Hence, we provide our own custom dataset for this purpose.

4.1 Image Capturing

We captured images across 80 different corridors of National Institute of Technology, Rourkela, India, out of which 59 and 21 corridors are used for training and testing purpose respectively. The images are captured by the UAV front

camera at a resolution of 320×180 . While preparing the dataset, it is made sure that the dataset covers all the possible positions across the whole length of the corridor. The height of the UAV is kept at approximately 1 meter. At a certain place inside the corridor, there different locations over a horizontal line, which is perpendicular to the CBL, are selected. These locations are mainly the center and two extreme sides of the corridor. At each location over the horizontal line, images are captured while the UAV is tilted in three different orientations: center, left, and right tilt. Hence, we will have 9 different images corresponding to a particular horizontal line. Possible scenarios are shown in Figure 2. These horizontal lines are chosen across the whole length of the corridor at certain intervals. However, these images do not provide any information regarding the CBL. Hence, for each image, a similar image is captured by placing two markers on the CBL of the corridor. These images are known as bisector images. Markers are placed on the floor by measuring the middle point between the two side walls. One marker is placed at the extreme end of the corridor, and its position remains the same for all the images. The second marker is placed somewhere inside the corridor, such that it will be visible on the captured image. We alter the position of the second marker to make it visible throughout the process of image capturing. Although the actual image and its corresponding bisector image vary slightly in terms of pixel values, their geometry, which holds key information regarding the corridor structure, is preserved. It may be noted that the bisector images do not correspond to the final dataset. These are only used for obtaining the target values for the actual images.

4.2 Labeled Data Generation

The bisector images are processed to detect the markers, and then these markers are connected by a red colored line, which forms the CBL on the image plane (Figure 3). The bisector images are then checked manually for any discrepancy (CBL is not drawn properly), and erroneous images are discarded from the dataset. It has been observed that when the UAV is on the left side of the CBL, this red line on the image plane forms an acute angle with the bottom image boundary, as shown in Figure 4(a). In case the UAV is on the right side of the CBL, the angle formed is obtuse (Figure 4(b)). When the UAV is at the center, it forms a right angle (Figure 4(c)). Hence, for the corresponding actual image in the dataset, these angles (in radians), are stored as the target values. It may be noted that these angles remain the same irrespective of the UAV tilt. The angles lie in the range $[0, 3.14]$. For safe localization of the UAV, always the goal is to keep the UAV at the center of the corridor. Alternatively, when the UAV is either on the left or right side of the CBL, our aim is to generate commands for the UAV such that this angle will shift towards the right angle. This labeled data will help in knowing the translational shift of the UAV from the CBL. However, it does not provide any information regarding the UAV tilt/orientation.

Once the UAV is at the center of the corridor over the CBL, we will try to measure the orientation of the UAV. It has been observed that when the UAV is at the center and aligned with the CBL, the red line on the bisector image



Fig. 2: Images as captured by the UAV front camera from 9 different possible alignments over a horizontal line perpendicular to the CBL. From top to bottom, the rows represent the images, when the UAV is at the center, extreme left and extreme right over the horizontal line, respectively. From left to right, the columns represent the orientations towards center, left and right, respectively.

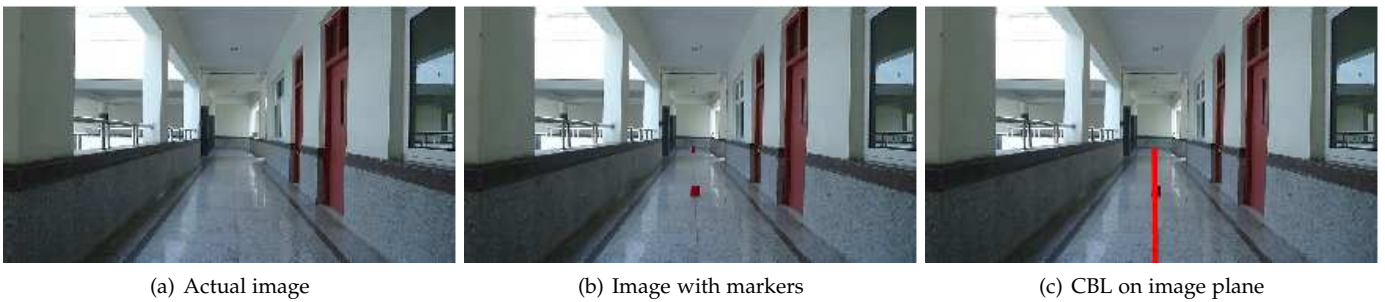


Fig. 3: Process of obtaining the CBL on the image plane using markers

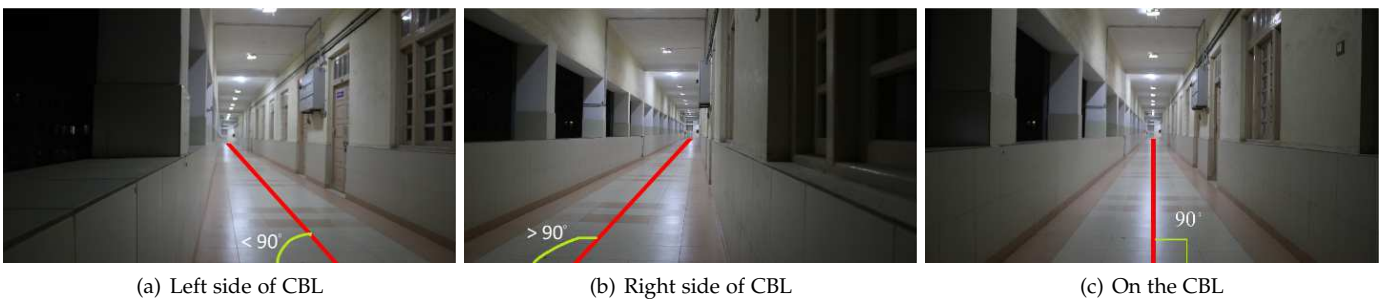


Fig. 4: Three different positions of the UAV over a horizontal line perpendicular to the CBL

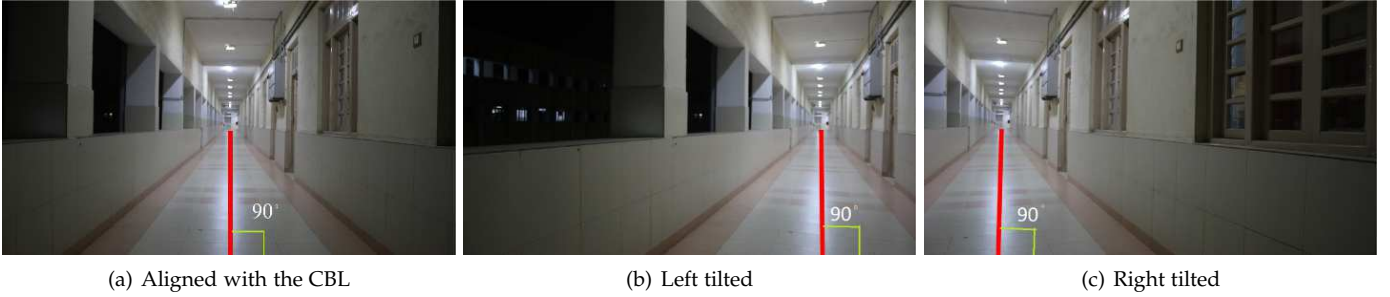


Fig. 5: Three different orientations of the UAV, when it is situated on the CBL

cuts the image plane vertically into two equal halves, as shown in Figure 5(a). However, when the UAV is at the center but left tilted, this red line although perpendicular to the bottom image boundary deviates from the center and cuts the image plane into two unequal halves with the left side having more area than the right side (Figure 5(b)). The opposite scenario holds true, when the UAV is at the center, but right tilted (Figure 5(c)). We calculate the number of pixels in the x-direction from the left image boundary to the vertical red line and normalize it with the image width to obtain the target value for the corresponding actual image in the dataset. The value lies in the range of $[0, 1]$. This normalized value is known as the pixel distance of the CBL. When the distance is 0.5, the UAV is properly aligned with the CBL. The UAV is right tilted when the distance is less than 0.5, and vice versa. Hence, for the corresponding actual image in the dataset, these distances, are stored as the target values for measuring the orientation. Always, the goal is to keep the UAV aligned with the CBL. Alternatively, when the UAV is at the center, and either left or right tilted, our aim is to generate commands for the UAV such that this distance will shift towards 0.5. This labeled data will help in knowing the rotational deviation of the UAV.

The dataset now contains two target values; (1) angle of the CBL (for rectifying the translational deviation), and (2) distance of the CBL (for rectifying the rotational deviation). Both target values can be utilized simultaneously in two similar DNNs to localize the UAV in corridor environments. We have shared this dataset as a public dataset, named NITRCorrV1 [9]. This dataset contains 35000 training and 600 testing images for angle, and 21000 training and 300 testing images for distance, and their corresponding target values.

5 DEEP NEURAL NETWORK FOR AUTONOMOUS UAV NAVIGATION

Our goal is to keep the UAV aligned with the CBL of the corridor throughout the process of navigation. This is a two-step process occurring consecutively; (1) Rectifying the translational deviation (side-wise variation) for bringing the UAV to center over the CBL, (2) Rectifying the rotational deviation (change in orientation) to align the UAV with the CBL, when the UAV is already at the center. Both processes are achieved by processing the images from the UAV front camera through pre-trained DNNs, that predict the deviations. Although the architecture of both the networks

remains same, the target output differs; one is for angle in radian and other is for normalized pixel distance. As the unit of both the target values (angle and pixel distance) are different, it is not feasible to train both the quantities simultaneously using the same network.

5.1 Network Structure

For both the tasks, we used some of the standard pre-trained models (AlexNet [31], VGGNet [32], InceptionNet [33], ResNet [34], DenseNet [35]) to train our custom dataset. The last fully connected layer of the pre-trained model is replaced by a few convolution layers to decrease the output feature map size. At the end of the network, one fully connected layer is appended to obtain 1×1 output. The input image resolution is 320×180 . Various networks that are used to train our dataset is shown in Table 1. The proposed network acts as a regression model, as the network directly predicts a numeric value, instead of a class. The same network is trained separately for translational deviation and rotational deviation, just by changing the target output. In case of translational deviation, the target is the angle (in radians) made by the CBL with bottom image boundary plane, and for rotational deviation, the target is a normalized pixel distance of the CBL from the left image boundary. The angle lies in the range $[0, 3.14]$ and the normalized pixel distance lies in the range of $[0, 1]$. A free body diagram of our proposed model is shown in Figure ??.

5.2 Loss Function

Accurate selection of a loss function plays an important role in carrying out any deep learning based optimization task. We have used the Mean Absolute Error (MAE) loss function to train our models. MAE is formulated as —

$$\text{MAE}(\hat{y}, y) = \frac{1}{n} \sum_{i=1}^n |\hat{y}_i - y_i| \quad (1)$$

Where, \hat{y} and y denote the list of predicted and target values for a mini batch of size n .

5.3 Training

Input Pre-processing. The proposed model accepts an input of resolution 320×180 . Before processing, the original BGR pixel values, which lie in the range $[0, 255]$, are first normalized to the range $[0, 1]$. Each of the Blue, Green and Red channels are then normalized by the

TABLE 1: Various pre-trained models and their augmented convolution layers to train our custom dataset. In the 2D convolution operation, $\text{Conv2d}(C_{in}, C_{out}, k \times k)$, C_{in} , C_{out} , and k represent the number of input channels, number of output channels, and kernel size respectively.

Input	Pre-trained Models	Augmented Convolution Layers	Augmented last Fully connected layer	Output layer
320 × 180	AlexNet [31]	no augmentation of convolution layer	4096 × 1	1 × 1
	VGG-16 [32]	Conv2d(512, 1024, 1 × 1) Conv2d(1024, 128, 5 × 5) Conv2d(128, 16, 1 × 1)	96 × 1	
	InceptionV3 [33]	Main: Conv2d(2048, 1024, 1 × 1) Conv2d(1024, 512, 2 × 2) Conv2d(512, 128, 3 × 3) Aux: Conv2d(768, 128, 4 × 4) Conv2d(128, 32, 2 × 2)	Main: 256 × 1 Aux: 640 × 1	
	ResNet-50 [34]	Conv2d(2048, 1024, 1 × 1)	96 × 1	
	ResNet-101 [34]	Conv2d(1024, 128, 5 × 5)		
	ResNet-152 [34]	Conv2d(128, 8, 1 × 1)		
	DenseNet-201 [35]	Conv2d(1920, 1024, 1 × 1) Conv2d(1024, 128, 5 × 5) Conv2d(128, 16, 1 × 1)	96 × 1	
	DenseNet-161 [35]	Conv2d(2208, 1024, 1 × 1) Conv2d(1024, 128, 5 × 5) Conv2d(128, 16, 1 × 1)		

corresponding mean ($\mu_b = 0.406, \mu_g = 0.456, \mu_r = 0.485$) and standard deviation ($\sigma_b = 0.225, \sigma_g = 0.224, \sigma_r = 0.229$) of the ImageNet classification dataset [36]. Prediction of translational deviation requires images from all possible locations of the corridor, however rotational deviation requires images when the UAV is at the center and tilted in all three orientations (left, right or center).

Parameter Initialization. The initial parameters of the networks remain same for both the tasks. MAE 1 is used as the loss function, while Stochastic Gradient Descent (SGD) [37] is used as the optimizer. Overfitting is handled by L_2 regularization. Initial Momentum is set to 0.9 and learning rate starts at 0.001.

Training is performed separately for the prediction of translational and rotational deviation. We used 9 different pre-trained networks (AlexNet, VGG-16, InceptionV3, ResNet-50, ResNet-101, ResNet-152, DenseNet-201, DenseNet-161) to train our model. Training is performed separately for each of the pre-trained networks. Learning rate is reduced by a factor of 5, if the training loss remained same for consecutive 5 iterations. The process of training continues, till the learning rate reaches 10^{-15} .

5.4 Control Command generation

When the UAV is properly aligned with the CBL of the corridor, there is minimal chance of collision. Depending on the predictions of both the networks, control commands are generated to localize the UAV along the CBL of the corridor. The images from the UAV front camera are continuously processed through the trained networks to maintain the UAV pose. Algorithm 1 depicts the flow for generating the control commands for UAV navigation through an indoor corridor.

6 EXPERIMENTS

This section presents a detailed analysis of all the experiments carried out for the task of UAV navigation inside indoor corridor environments, using DNNs. The test sets of our custom dataset, NITRCorrV1, is used for

Algorithm 1: Control command generation

Input: Image From UAV front camera: img
Output: UAV direction: $[pitch, roll, yaw]$

- 1 $angle = \text{TrainedModelForAngle}(img)$
- 2 **if** $angle$ out of bound for continuously 1 second **then**
- 3 | Land the UAV
- 4 **if** $angle \approx 90^\circ$ **then**
- 5 | $dist = \text{TrainedModelForDistance}(img)$
- 6 | **if** $dist \approx 0.5$ **then**
- 7 | Actuate UAV in Pitch Forward
- 8 | **else if** $dist < 0.5 - \delta$ **then**
- 9 | Actuate UAV in Yaw Left until $dist \approx 0.5$
- 10 | **else**
- 11 | Actuate UAV in Yaw Right until $dist \approx 0.5$
- 12 **else if** $angle < 90^\circ - \delta$ **then**
- 13 | Actuate UAV in Roll Right until $angle \approx 90^\circ$
- 14 **else**
- 15 | Actuate UAV in Roll Left until $angle \approx 90^\circ$
- 16 **return** $[pitch, roll, yaw]$

validation purpose. We also show the system setup and hardware platform on which the experiments are being carried out. Finally, we show the results of our proposed navigation algorithm in real-world UAV flight experiments.

6.1 System Setup

We used PyTorch deep learning library to implement our deep networks. Training is performed with GTX 1080 Ti graphics card, which has a memory of 11GB. ILSVRC [38] pretrained weights are used for initializing the standard state-of-the-art networks. Weights for other convolution layers are initialized from a normal distribution $\mathcal{N}(0, \sqrt{2/ck^2})$, where k represents the filter size and c is the number of output channels of the convolution operation.

6.2 Evaluation Metrics

Evaluation is done on the NITRCorrV1 labeled test set, which contains 600 images for translational and 300 images

for rotational deviation, respectively. Test input images are preprocessed using the same procedure as the training images. We used three different evaluation metrics to validate our proposed DNN models.

(a) Mean Squared Error : $MSE(\hat{y}, y) = \frac{1}{n} \sum_{i=1}^n (\hat{y}_i - y_i)^2$

(b) Mean Absolute Error : $MAE(\hat{y}, y) = \frac{1}{n} \sum_{i=1}^n |\hat{y}_i - y_i|$

(c) Mean Relative Error : $MRE(\hat{y}, y) = \frac{1}{n} \sum_{i=1}^n \frac{|\hat{y}_i - y_i|}{y_i}$

Where, \hat{y} and y denote the list of predicted and target values for a mini batch of size n .

6.3 Results and Discussion

We compared the results of our proposed model using 9 different augmented pretrained networks, as given in Table 1. The comparison is done separately for translational and rotational deviation using separate test sets. Table 2 and Table 3 show the quantitative comparison results for both the tasks. It can be viewed that DenseNet-161 performs superior as compared to other pretrained networks for both the tasks in terms of all the evaluation metrics. Hence, for real-time navigation experiments, we used DenseNet-161 pretrained network to navigate the UAV in corridor environments. Location wise qualitative comparison results using DenseNet-161 pretrained network are shown in Tables 6 and 7.

TABLE 2: Evaluation metrics for the prediction of translational deviation of the UAV using 9 different pretrained networks over 600 test images.

Pre-trained Model	MSE	MAE	MRE
AlexNet	0.21997	1.72831	1.39280
VGG-16	0.47318	2.84597	2.41795
InceptionV3	0.11929	1.44906	1.20959
ResNet-50			
ResNet-101	0.11103	1.46875	1.17946
ResNet-152	0.11032	1.41558	1.16529
DenseNet-201	0.12383	1.79144	1.42709
DenseNet-161	0.05791	1.32693	1.08712

TABLE 3: Evaluation metrics for the prediction of rotational deviation of the UAV using 9 different pretrained networks over 300 test images.

Pre-trained Model	MSE	MAE	MRE
AlexNet	5.5677	27.0064	54.1467
VGG-16			
InceptionV3	0.0687	3.1364	10.4852
ResNet-50	0.0473	2.7485	9.0729
ResNet-101	0.1186	4.2163	14.6806
ResNet-152	0.06617	3.4258	10.8230
DenseNet-201	0.0828	3.6442	12.1421
DenseNet-161	0.0326	2.5060	1.557

6.4 Real World Navigation Experiments

We tested our deep learning based UAV navigation algorithm in real-world indoor corridors. Parrot A.R.Drone quadcopter is used to validate the experiments. It has a static front camera, which provides video feed at 30 frames per second (fps). The UAV is capable of producing a fisheye video (92° field of view) with a resolution of 640 × 480. Before processing the images through the DNN, the fisheye images are converted to their rectilinear equivalent. Also,

the images are downsampled to 320 × 180, which is the default input to the proposed deep learning model. The UAV is connected to a ground-based system, where the deep learning model is running, though wireless LAN and communication take place using the Robot Operating System (ROS). Image frames from the UAV front camera are passed continuously through the ROS to the deep learning system. Image transmission delay through ROS is about 0.21s. Our deep learning model prediction takes about 0.08s for measuring both translational and rotational deviation simultaneously. The system then generates the appropriate control command using Algorithm 1, and forwards it to the UAV through the ROS. The UAV internal PID controller is then responsible for executing the command and maintaining safe UAV pose during its navigation. It may be noted that apart from our network prediction, different factors, such as control and state estimation affect the actual UAV flight in real-world scenarios. Because of the unstable and fluctuating state estimation of Parrot drone, we cannot employ the positional feedback in path planning, which sometimes deteriorates the whole navigation process. It is observed that our proposed DNN based navigation algorithm works with good accuracy in most of the corridors.

7 CONCLUSION

In this work, we proposed a DNN based UAV localization algorithm, which enables the UAV to navigate safely inside corridors environments. Unlike the previous methods, where the deep models were designed to predict flight commands directly, our proposed method makes use of an important characteristic of a corridor, the CBL, to generate commands. We designed a single deep network and trained it separately for two tasks; (a) prediction of translational deviation of the UAV from the CBL, and (b) prediction of rotational deviation of the UAV with respect to the CBL. These two predictions are then used to design a navigation algorithm, which enables the UAV to maintain a safe pose inside the corridor. We also provide a new corridor dataset, NITRCorrV1, in which the corridor images are labeled in terms of translational and rotational deviation values. Our proposed navigation algorithm is capable of navigating a UAV inside real-world corridor environments with good accuracy.

REFERENCES

- [1] K. Gryte, J. M. Hansen, T. Johansen, and T. I. Fossen, "Robust navigation of UAV using inertial sensors aided by UWB and RTK GPS," in *AIAA Guidance, Navigation, and Control Conference*, 2017, pp. 1035–1050.
- [2] M. Y. Chen, D. H. Edwards, E. L. Boehmer, N. M. Eller, J. T. Slack, C. R. Speck, S. M. Brown, H. G. Williams, S. H. Wilson, C. S. Gillum *et al.*, "Designing a spatially aware and autonomous quadcopter," in *Systems and Information Engineering Design Symposium*. IEEE, 2013, pp. 213–218.
- [3] J. Engel, J. Sturm, and D. Cremers, "Camera-based navigation of a low-cost quadcopter," in *IEEE/RSJ International Conference on Intelligent Robots and Systems*, ser. IROS. IEEE, 2012, pp. 2815–2821.
- [4] —, "Scale-aware navigation of a low-cost quadcopter with a monocular camera," *Robotics and Autonomous Systems*, vol. 62, no. 11, pp. 1646–1656, 2014.

Fig. 6: Qualitative performance evaluation of translational deviation for different corridor locations of National Institute of Technology, Rourkela, India. Ground truth and predicted values are given in degree. GT: Ground truth, PR: Predicted.

TIIR Building	Physics Department	Life Science Department	Computer Science Department
			
GT: 90.720° PR: 90.303°	GT: 47.055° PR: 46.707°	GT: 90.000° PR: 91.142°	GT: 136.507° PR: 135.253°

Fig. 7: Qualitative performance evaluation of rotational deviation for different corridor locations of National Institute of Technology, Rourkela, India. Ground truth and predicted values are in the range [0, 1]. GT: Ground truth, PR: Predicted.

TIIR Building	Physics Department	Life Science Department	Computer Science Department
			
GT: 0.488 PR: 0.491	GT: 0.805 PR: 0.808	GT: 0.547 PR: 0.528	GT: 0.167 PR: 0.163

- [5] I. Sa, H. He, V. Huynh, and P. Corke, "Monocular vision based autonomous navigation for a cost-effective MAV in GPS-denied environments," in *IEEE/ASME International Conference on Advanced Intelligent Mechatronics*. IEEE, 2013, pp. 1355–1360.
- [6] M. Achtelik, A. Bachrach, R. He, S. Prentice, and N. Roy, "Stereo vision and laser odometry for autonomous helicopters in GPS-denied indoor environments," in *SPIE Defense, Security, and Sensing*. International Society for Optics and Photonics, 2009, pp. 733 219–733 228.
- [7] K. McGuire, G. de Croon, C. De Wagter, K. Tuyls, and H. Kappen, "Efficient optical flow and stereo vision for velocity estimation and obstacle avoidance on an autonomous pocket drone," *IEEE Robotics and Automation Letters*, vol. 2, no. 2, pp. 1070–1076, 2017.
- [8] H. Qin, Y. Bi, K. Z. Ang, K. Wang, J. Li, M. Lan, M. Shan, and F. Lin, "A stereo and rotating laser framework for UAV navigation in GPS denied environment," in *IEEE Annual Conference of the Industrial Electronics Society*. IEEE, 2016, pp. 6061–6066.
- [9] "Corridor Dataset for UAV Navigation," <http://www.nitrkl.ac.in/docs/CS/Database/Dataset%20for%20UAV%20Navigation%20inside%20corridor%20environments.htm>.
- [10] S. Grzonka, G. Grisetti, and W. Burgard, "Autonomous indoor navigation using a small-size quadrotor," in *Workshop Proceedings SIMPAR*, 2008, pp. 455–463.
- [11] A. Bachrach, S. Prentice, R. He, and N. Roy, "RANGE—Robust autonomous navigation in GPS-denied environments," *Journal of Field Robotics*, vol. 28, no. 5, pp. 644–666, 2011.
- [12] N. Gageik, P. Benz, and S. Montenegro, "Obstacle detection and collision avoidance for a UAV with complementary low-cost sensors," *IEEE Access*, vol. 3, pp. 599–609, 2015.
- [13] G. C. S. Cruz and P. M. M. Encarnação, "Obstacle avoidance for unmanned aerial vehicles," *Journal of Intelligent & Robotic Systems*, vol. 65, no. 1–4, pp. 203–217, 2012.
- [14] A. Stubblebine, B. Redmond, B. Feie, and E. Kivelevitch, "Laser-guided quadrotor obstacle avoidance," in *AIAA Infotech @ Aerospace*. AIAA, 2015, pp. 2026–2037.
- [15] J. F. Roberts, T. Stirling, J.-C. Zufferey, and D. Floreano, "Quadrotor using minimal sensing for autonomous indoor flight," in *European Micro Air Vehicle Conference and Flight Competition (EMAV2007)*, no. LIS-CONF-2007-006, 2007.
- [16] J. Martínez-Carranza, E. O. Garcia, H. J. Escalante, and W. Mayol-Cuevas, "Towards autonomous flight of low-cost MAVs by using a probabilistic visual odometry approach," in *Advances in Artificial Intelligence and its Applications*. Springer, 2015, pp. 560–573.
- [17] T. Mori and S. Scherer, "First results in detecting and avoiding frontal obstacles from a monocular camera for micro unmanned aerial vehicles," in *IEEE International Conference on Robotics and Automation*. IEEE, 2013, pp. 1750–1757.
- [18] S. Saha, A. Natraj, and S. Waharte, "A real-time monocular vision-based frontal obstacle detection and avoidance for low cost UAVs in GPS denied environment," in *IEEE International Conference on Aerospace Electronics and Remote Sensing Technology*. IEEE, 2014, pp. 189–195.
- [19] C. Wang, W. Liu, and M. Q.-H. Meng, "Obstacle avoidance for quadrotor using improved method based on optical flow," in *IEEE International Conference on Information and Automation*. IEEE, 2015, pp. 1674–1679.
- [20] S. Weiss, M. W. Achtelik, S. Lynen, M. Chli, and R. Siegwart, "Real-time onboard visual-inertial state estimation and self-calibration of MAVs in unknown environments," in *IEEE International Conference on Robotics and Automation*, ser. ICRA. IEEE, 2012, pp. 957–964.
- [21] Z. He, R. V. Iyer, and P. R. Chandler, "Vision-based UAV flight control and obstacle avoidance," in *American Control Conference*. IEEE, 2006, pp. 2166–2170.
- [22] A. Lioulemes, G. Galatas, V. Metsis, G. L. Mariottini, and F. Makedon, "Safety challenges in using AR.drone to collaborate with humans in indoor environments," in *International Conference on Pervasive Technologies Related to Assistive Environments*. ACM, 2014, pp. 33–36.
- [23] R. P. Padhy, F. Xia, S. K. Choudhury, P. K. Sa, and S. Bakshi, "Monocular vision aided autonomous UAV navigation in indoor corridor environments," *IEEE Transactions on Sustainable Computing*, 2018.
- [24] D. K. Kim and T. Chen, "Deep neural network for real-time

- autonomous indoor navigation," *arXiv preprint arXiv:1511.04668*, 2015.
- [25] R. P. Padhy, S. Verma, S. Ahmad, S. K. Choudhury, and P. K. Sa, "Deep neural network for autonomous uav navigation in indoor corridor environments," *Procedia computer science*, vol. 133, pp. 643–650, 2018.
- [26] C. Bills, J. Chen, and A. Saxena, "Autonomous MAV flight in indoor environments using single image perspective cues," in *IEEE international conference on Robotics and automation (ICRA)*. IEEE, 2011, pp. 5776–5783.
- [27] A. S. Etienne, R. Maurer, J. Georgakopoulos, and A. Griffin, "Dead reckoning (path integration), landmarks, and representation of space in a comparative perspective," *Wayfinding behavior : cognitive mapping and other spatial processes*, pp. 197–228, 1999.
- [28] A. Chavez and D. Gustafson, "Vision-based obstacle avoidance using SIFT features," in *Advances in Visual Computing*. Springer, 2009, pp. 550–557.
- [29] A. Quattoni and A. Torralba, "Recognizing indoor scenes," in *2009 IEEE Conference on Computer Vision and Pattern Recognition*, 2009, pp. 413–420.
- [30] R. Huitl, G. Schroth, S. Hilsenbeck, F. Schweiger, and E. Steinbach, "TUMindoor: An extensive image and point cloud dataset for visual indoor localization and mapping," in *2012 19th IEEE International Conference on Image Processing*, 2012, pp. 1773–1776.
- [31] A. Krizhevsky, I. Sutskever, and G. E. Hinton, "Imagenet classification with deep convolutional neural networks," in *Advances in neural information processing systems*, 2012, pp. 1097–1105.
- [32] K. Simonyan and A. Zisserman, "Very deep convolutional networks for large-scale image recognition," *arXiv preprint arXiv:1409.1556*, 2014.
- [33] C. Szegedy, W. Liu, Y. Jia, P. Sermanet, S. Reed, D. Anguelov, D. Erhan, V. Vanhoucke, and A. Rabinovich, "Going deeper with convolutions," in *Proceedings of the IEEE conference on computer vision and pattern recognition*, pp. 1–9.
- [34] K. He, X. Zhang, S. Ren, and J. Sun, "Deep residual learning for image recognition," in *Proceedings of the IEEE Conference on Computer Vision and Pattern Recognition*, 2016, pp. 770–778.
- [35] G. Huang, Z. Liu, K. Q. Weinberger, and L. van der Maaten, "Densely connected convolutional networks," *arXiv preprint arXiv:1608.06993*, 2016.
- [36] J. Deng, W. Dong, R. Socher, L.-J. Li, K. Li, and L. Fei-Fei, "Imagenet: A large-scale hierarchical image database," in *IEEE Conference on Computer Vision and Pattern Recognition*. IEEE, 2009, pp. 248–255.
- [37] L. Bottou, "Large-scale machine learning with stochastic gradient descent," in *19th International Conference on Computational Statistics*. Springer, 2010, pp. 177–186.
- [38] O. Russakovsky, J. Deng, H. Su, J. Krause, S. Satheesh, S. Ma, Z. Huang, A. Karpathy, A. Khosla, M. Bernstein *et al.*, "ImageNet large scale visual recognition challenge," *International Journal of Computer Vision*, vol. 115, no. 3, pp. 211–252, 2015.